PHYSICAL REVIEW B **80**, 241313(R) (2009)

Temperature dependence of the crossover between the near-infrared Er and defect-related photoluminescence bands of Ge-rich Er-doped SiO_2 layers

A. Kanjilal,* L. Rebohle, S. Prucnal, M. Voelskow, W. Skorupa, and M. Helm
Institute of Ion Beam Physics and Materials Research, Forschungszentrum Dresden-Rossendorf, P.O. Box 51 01 19, 01314 Dresden, Germany

(Received 25 November 2009; published 30 December 2009)

Temperature-dependent photoluminescence of Ge-rich SiO_2 in the presence or absence of Er shows a crossover between defect-related (15–150 K) and Er-related (150–295 K) emission within 1525 and 1440 nm. The origin of the near-infrared defect-related bands is discussed in the light of recombination of localized excitons in luminescence centers at the Ge cluster/SiO_2 interface. Time-resolved photoluminescence further enables us to illustrate the observed 1.53 μm Er emission above 150 K in terms of a phonon-assisted nonradiative energy-transfer process from the luminescence centers to the Er^{3+} ions.

DOI: 10.1103/PhysRevB.80.241313 PACS number(s): 78.67.Bf, 78.55.−m, 78.66.Jg

Bulk silicon and germanium, basic elements in microelectronic industries, are not suitable for photonic and optoelectronic applications because of their indirect band gaps. However, the situation has remarkably been improved by using their nanostructures. Owing to the tunable luminescence properties, crystalline, and amorphous forms of Si or Ge nanostructures dispersed in a SiO_2 layer have further been employed for enhancing the 1.53 μm Er photoluminescence (PL) intensity when excited with a wavelength nonresonant to the Er emission.[1–5] In contrast to Ge nanoclusters, much research has been devoted so far to the systems containing Si nanocrystals (NCs) in Er-doped SiO_2 due to their extraordinary performance in amplifying the 1.53 μm Er PL.[1–3] However, in any case the mechanism is governed by an energy-transfer process from optically excited semiconductor nanocluster to the Er^{3+} ions, which decay radiatively via an intra-4f $^4I_{13/2} \rightarrow {}^4I_{15/2}$ transition. Moreover, defects residing at the NC/SiO_2 interface have also been invoked in transferring energy to the Er^{3+} ions for a multifold improvement of the 1.53 μm Er PL.[6] It has been demonstrated by Heng *et al.*[4] that the amorphous Ge nanoclusters play the key role in transferring energy to the Er^{3+} ions, while quite recently a defect-related model has also been proposed.[7] Only few groups[7,8] paid attention on the temperature-dependent PL properties of such systems to understand the Er excitation process, while it is essential to exploit its potential and to improve the 1.53 μm Er PL intensity for fabricating complementary metal-oxide semiconductor compatible waveguide amplifiers, solar cells, and lasers operating at this telecommunication wavelength.

In this Rapid Communication, we report the evolution of the 1.53 μm Er PL from a Er:Ge-NC:SiO_2 layer at room temperature (RT) under different Er concentrations (C_{Er}) and Ge concentrations (C_{Ge}), and we correlate these results with the corresponding microstructural properties. By investigating the temperature dependence of the infrared (IR) PL, here we demonstrate a *crossover* between a pulsed (15–150 K) and continuous (150–295 K) regime close to the 1.53 μm Er emission. In particular, independent of the presence of Er in Ge-rich SiO_2 a weak variation in intensity and peak position is observed below 150 K for two PL bands, called $P1$ and $P2$ around 1525 and 1440 nm, respectively. Clear appearance of the typical 1.53 μm Er emission above 150 K with a concomitant quenching of both $P1$ and $P2$, especially the former one with a completely different line shape, is recorded. In our knowledge, such an intriguing PL behavior has *never* been reported before for Er:Ge-NC:SiO_2. The correlation between $P1$ and the 1.53 μm Er PL is discussed further using time-resolved PL measurements.

130 keV Ge ions were implanted with fluences of 2×10^{16}–6×10^{16} ions/cm^2 (maximum C_{Ge} in between 3.5% and 11.1% at $R_p \sim 112$ nm, derived from SRIM-2006 calculations[9]) into a 200 nm thick thermally grown SiO_2 layer on Si(100) wafers. The samples were annealed at 950 °C for 60 min. Subsequently, 250 keV Er ions were implanted with fluences of 1×10^{15}–5×10^{15} ions/cm^2 (maximum C_{Er} of 0.3–1.4% at $R_p \sim 115$ nm), followed by annealing at 900 °C for 30 min to remove ion-beam-induced defects and to activate Er^{3+} ions.[10] In order to follow the PL response and to understand the contribution of Ge and Er, two independent samples were prepared by implanting either Ge or Er ions in a SiO_2 layer followed by annealing at 950 °C for 60 min or at 900 °C for 30 min, respectively.

Depth profiles of the samples were examined by Rutherford backscattering spectrometry. Cross-sectional transmission electron microscopy (XTEM) images were taken with a FEI TITAN 80-300 S/TEM instrument operating at 300 keV. The PL measurements were carried out at various temperatures in the range of 15–295 K by mounting the investigating sample in a closed-cycle helium cryostat, while the samples were excited with the 532 nm line of a Nd:YAG laser with a power of 5–200 mW. The PL signals were analyzed with a single grating monochromator (TRIAX-550) and detected by an InGaAs detector in the IR region with a standard lock-in technique where the laser beam was modulated by a rotating chopper. The visible range PL spectra were recorded using a charge-coupled camera device or by a photomultiplier (Hamamatsu H7732-10), while the latter one was further employed to analyze the time-resolved PL dynamics in combination with a photon counting system.

Both panels of Fig. 1 display the visible and IR PL spectra of the SiO_2 layers containing 3.5% Ge with and without Er, respectively, when the samples were excited with a moderate (5 mW) power. As apparent, the 625 nm PL intensity and the spectral shape do not change by Er doping. The PL spectrum has also been recorded for 7.4% Ge, containing larger Ge

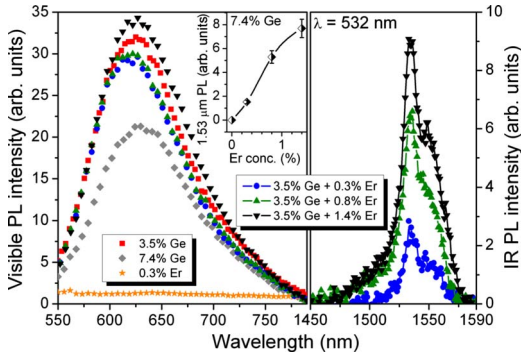

FIG. 1. (Color online) (Left panel) RT visible range PL spectra of the SiO_2 layers containing only 3.5% Ge (■), 7.4% Ge (♦), and 0.3% Er (★) and the spectra for 3.5% Ge with 0.3% Er (●), 0.8% Er (▲), and 1.4% Er (▼). (Right panel) The 1.53 μm Er emission for 0.3%, 0.8%, and 1.4% Er in the presence of 3.5% Ge. The inset (left panel) displays variation of the 1.53 μm Er PL intensity as a function of Er concentration for 7.4% Ge.

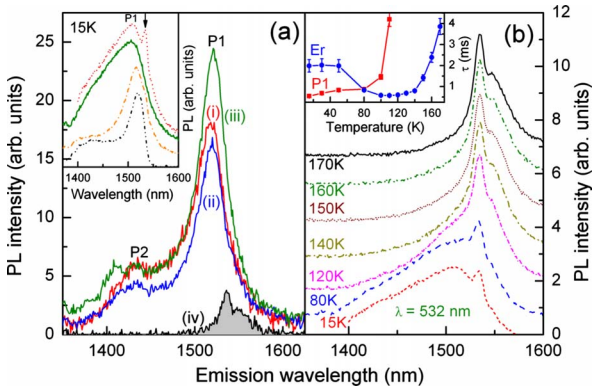

FIG. 2. (Color online) (a) IR PL spectra recorded at 15 K for (i) 3.5% Ge and (ii) 7.4% Ge only, and at (iii) 15 K and (iv) 295 K for 3.5% Ge+1.4% Er; inset shows the PL spectra for 3.5% Ge +1.4% Er at 15 K with excitation powers of 5 mW (dashed-double-dotted curve), 20 mW (dashed-dotted curve), and 200 mW (dashed curve) where the spectrum for 3.5% Ge+0.3% Er with an excitation power of 200 mW is shown by solid curve. (b) The PL spectra for 3.5% Ge+1.4% Er at various temperatures with a 200 mW excitation power; inset shows temperature dependence of τ_{P1} (■) and τ_{Er} (●).

NCs (average diameter of ~9.4 nm).[11] The superimposed PL spectra do not show any significant peak shifting with varying C_{Ge}, while hardly any change in the PL decay time (~540 μs) was registered, even after Er doping, confirming that the 625 nm PL is not associated with the quantum confinement in Ge NCs.[12–14] As expected, only Er-doped SiO_2 does not give any visible PL as the 532 nm line is nonresonant to the $4f$ levels of Er^{3+}.[15] Based on prior studies[16] the 625 nm emission is assigned to the nonbridging oxygen-hole center ($O_3 \equiv Si\text{-}O\cdot$). The 1.53 μm Er PL was also absent in $Er:SiO_2$, whereas a typical 1.53 μm Er emission[10] was recorded at RT in the presence of excess Ge (Fig. 1). In fact, the 1.53 μm Er PL intensity increases with increasing C_{Er} (right panel in Fig. 1). A similar trend is obtained also for 7.4% Ge (inset, left panel in Fig. 1). To gain insights into such a C_{Er}-dependent variation in the 1.53 μm Er PL intensity, we investigate the corresponding microstructures[11,17] that reflect two parallel processes: (i) fragmentation and/or amorphization of Ge NCs with increasing C_{Er} and (ii) the formation of Er composites either by increasing C_{Er} or annealing temperature. Since Ge NCs were gradually damaged by Er doping,[17] the observed enhancement of the 1.53 μm PL intensity in the absence of any significant modification in 625 nm PL cannot be explained in terms of an energy-transfer process from Ge NC to the Er^{3+} ions. Instead, it is reasonable to interpret the observed phenomenon in the framework of a Ge-related-defect induced excitation of the Er^{3+} ions.

In order to explore the mechanisms, the temperature dependence of the IR PL spectra was examined for samples containing either only 3.5% Ge (S_{Ge}) or 3.5% Ge codoped with 1.4% Er (S_{Ge+Er}). Well-resolved fine structures were recorded by decreasing temperature down to 15 K. Interestingly, two clear bands $P1$ and $P2$ were observed at low temperatures within 1525–1440 nm in both Er-doped or undoped Ge-NCs:SiO_2. The key finding is the complete disappearance of these peaks beyond 150 K in S_{Ge}, while a typical 1.53 μm Er PL is appeared above 150 K in S_{Ge+Er}. Additionally, the 1.53 μm Er PL intensity remains constant within 15% up to RT. To shed light on the origin of $P1$ ($P2$), we also verified low-temperature PL response for 7.4% Ge, even by changing C_{Er}. For instance, the PL spectra for (i) 3.5% and (ii) 7.4% Ge at 15 K, and those for S_{Ge+Er} at (iii) 15 K and (iv) RT are exhibited in Fig. 2(a). Close inspection reveals that the spectral shape in (iii) does not resemble the 1.53 μm Er emission at RT in (iv) for S_{Ge+Er}. We should emphasize that except lower PL intensity and the reduction in the full width at half-maximum with respect to (i), no discernible change in spectral shape and position is observed in (ii). Since Ge NCs are systematically modified by Er doping,[17] such a sharp and identical appearance of $P1$ in the presence or absence of Er is unlikely from the quantum confinement standpoints.[12–14] These peaks are basically associated with defect-related luminescence centers (LCs) at the Ge cluster/SiO_2 interface—this will be clarified in the following where the surface-to-volume ratio of Ge clusters plays an important role in controlling their intensities.

The inset of Fig. 2(a) exhibits the variation of the spectral shape of S_{Ge+Er} at 15 K with increasing laser power from 5 to 200 mW. Discernibly, while $P1$ and $P2$ are overlapped at 200 mW, the 1.53 μm Er PL is pronounced with increasing laser power. Close inspection reveals a blueshift of the most prominent peak $P1$ with increasing excitation power, which can be tentatively attributed to a competition between localized radiative recombination and Auger recombination.[18] The 1.53 μm Er emission is marked by downward arrow (↓). To elucidate its origin, we have taken a similar spectrum at 15 K for the sample containing 0.3% Er instead of 1.4% Er in Ge-NCs:SiO_2 (solid curve). The absence of the 1.53 μm Er PL in case of 0.3% Er suggests that the Er peak in S_{Ge+Er} is associated with an excitation of the Er^{3+} ions, which are staying apart from Ge clusters. In fact, the 1.53 μm Er PL was also observed in $Er:SiO_2$ for such a high excitation power. It seems that the higher-lying states of Er^{3+} are populated when the samples are excited strongly, which subsequently relax down to the first excited state before making $^4I_{13/2} \rightarrow {}^4I_{15/2}$ transition in Er^{3+}.

Since both $P1$ and the 1.53 μm Er PL are visible at 15 K in S_{Ge+Er}, we monitor these bands using such a high excitation power as a function of measuring temperature (T) to clearly demonstrate the relative change in their intensities [Fig. 2(b)] and to extract the respective decay times such as τ_{P1} and τ_{Er} (see the inset). Closer view of the IR bands provides evidence of T-dependent gradual appearance of a typical 1.53 μm Er PL with higher intensity at the expense of $P1$ ($P2$) above 150 K, which fits well with an energy-transfer process from $P1$ to the Er^{3+}. But we found that τ_{P1} increases gradually from 544 μs to 4.2 ms with increasing T up to 110 K, while with an initial halt at ~2 ms up to 50 K τ_{Er} decreases fast with increasing T. After reaching its minimum (574 μs) at 110 K, τ_{Er} again increases gradually up to 2.4 ms at 170 K due to the thermal redistribution over the Stark levels.[8] These phenomena are consistent with lower Er content, too. Note that the PL characteristics are determined by two recombination mechanisms such as radiative (with time τ_R) and nonradiative (with time τ_{NR}), while the PL decay rate ($\Gamma_{PL}=1/\tau_{PL}$) is defined by the sum of radiative ($\Gamma_R=1/\tau_R$) and nonradiative ($\Gamma_{NR}=1/\tau_{NR}$) rates.[19] In addition, the quantum yield (Γ_R/Γ_{PL}), proportional to the PL intensity provides the *weight* of the radiative recombination process. Hence, the T-dependent quenching of $P1$ with concomitant rise in τ_{P1} [Fig. 2(b)] can only be discussed in the light of an energy transfer due to the strong coupling between $P1$ ($P2$) and the Er^{3+} ions.[8] Based on this model, the luminescence appears from those LCs which are not coupled to Er, while the LCs that do couple to the Er^{3+} ions cannot emit any light. In fact, the increase in τ_{P1} may be associated with an interaction of phonons,[20] which as a consequence reduces the excitation cross section of the LCs.

So far the Förster-type[21] Coulomb interaction theory has been employed to interpret the energy transfer either between rare-earth ions[19] or NCs.[22] In fact, the Förster theory is the basis of the fluorescent resonant energy transfer (FRET) where the transfer rate (Γ_F) between the donor and acceptor (with an intermediate distance R) is inversely proportional to R^6; see Ref. 21 for details. Auger-like short-range[3] energy-transfer process is unexpected in our system as the nanoclusters of Ge and Er composites are staying apart from each other for 1.4% Er in Ge-NCs:SiO_2.[17] Since both Ge and Si have an indirect band gap, it is expected that Ge clusters hold the similar screening property as for Si NCs (Ref. 22) and, therefore, will not allow FRET to the Er located near the surface [like for 0.3% Er (Ref. 17)]. Although the FRET is mainly active in NCs with direct band gap,[22] it was presumed earlier that a slow FRET can also participate in transferring energy from Si NCs to the distant Er^{3+} ions.[10,23] Since LCs in our system are located at the Ge cluster/SiO_2 interface and separated from the active Er sites typically by ~5 nm for 1.4% Er,[17] it is straightforward to assume that the LCs are acting like dipolar donors and can transfer energy nonradiatively to the Er^{3+} (acceptor) by strong dipole-dipole coupling.[22] Note that Fig. 1 is plotted for moderate (5 mW) excitation power where direct excitation of the free Er^{3+} ions is not possible. Clearly, the 1.53 μm Er PL is mainly concerned with FRET, which is enhanced by increasing C_{Er}. We further monitored T-dependent variation of the maximum peak position (λ_{max}) and the maximum PL intensity (I_{max}) of

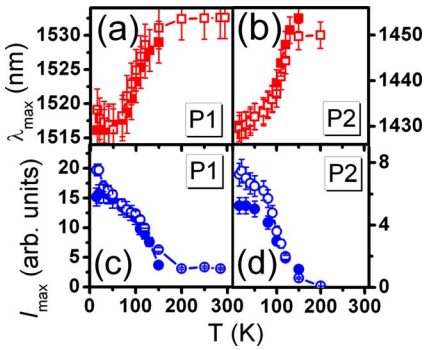

FIG. 3. (Color online) Shift in λ_{max} of (a) $P1$ and (b) $P2$ and variation of I_{max} of (c) $P1$ and (d) $P2$ are shown for only 3.5% Ge (lines plus filled symbols) and for the 3.5% Ge codoped with 1.4% Er (lines plus open symbols).

$P1$ ($P2$) for S_{Ge+Er} (Fig. 3). The observed redshift of $P1$ ($P2$) in the presence or absence of Er in Ge-rich SiO_2 can be explained in terms of an electron-phonon coupling in LCs. In fact, this redshift is essential for conducting well-known phonon-assisted FRET in presence of Er,[19,24] which gives an modified expression of Γ_F as $\Gamma_F=\Gamma_{PL}(R_0/R)^6\exp(-\beta\Delta E)$, where R_0 is the distance at which the transfer rate and the PL rate are equal; β depends on the electron-phonon coupling strength and ΔE depends on spectral overlapping. With increasing T, we believe that phonons not only assist in accelerating the FRET from $P1$ ($P2$) to the Er^{3+} ions, but also initiate nonradiative energy-back-transfer process from the Er^{3+}, thereby decreasing τ_{Er} [Fig. 2(b)]. In addition, soon after the complete disappearance of $P1$ ($P2$) above 150 K, the nonradiative channels of the Er^{3+} are eventually reduced with a further increase in T, giving an increase in τ_{Er} (Fig. 2).

The above assertion of considering $P1$ and $P2$ as LCs will be justified now. To evaluate whether they are originating from dislocations of the Si substrate,[25] we carried out low-temperature PL measurements on an unimplanted SiO_2 layer. The absence of $P1$ ($P2$) confirms that the impurities in S_{Ge} or in S_{Ge+Er} are mainly responsible behind the observed PL. We carefully analyze the microstructures by XTEM showing Ge NCs only in SiO_2.[17] Since Ge NCs are amorphized by 1.4% Er doping,[17] we can discard the involvement of dislocation in Ge clusters. The variation of λ_{max} [Figs. 3(a) and 3(b)] also does not follow the Varshni relationship, $E_g^{Si}=1155-7.02\times10^{-4}\ T^2/(T+1108)$,[26] which again confirms that both $P1$ and $P2$ are not correlated with Si band edges. In fact, they resemble the defect-related PL from Ge nanoclusters on Si,[18] whereas the corresponding peak positions are different from that of ours, possibly due to the variation of the surrounding matrix. As the peak maxima remain unchanged [Fig. 2(a)] irrespective of the strain in Ge NCs for 3.5% Ge (compressive) and 7.4% Ge (tensile),[11] we can also rule out the involvement of strain on the observed luminescence. Clearly, T-dependent change in $P1$ ($P2$) peak position and the corresponding PL quenching (Fig. 3) can only be justified in terms of thermal activation of localized excitons in the defect-related LCs, which are definitely different from that of the Ge-related oxygen-deficiency centers[11,27] as the latter one can be excited optically only by ultraviolet light.[28]

According to our model, the electrons and holes are con-

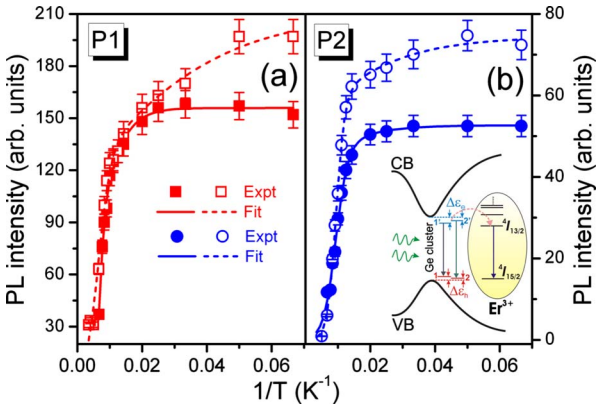

FIG. 4. (Color online) Arrhenius plots of the temperature-dependent PL intensities of (a) $P1$ and (b) $P2$ for only 3.5% Ge (filled symbols) and for the 3.5% Ge+1.4% Er (open symbols). The fitted results are superimposed for clarity where the fits for S_{Ge} and $S_{\mathrm{Ge+Er}}$ are projected by solid lines and dashed lines, respectively. Inset of (b) shows the schematic view of the processes in luminescence centers with states $\Delta\varepsilon_e$ and $\Delta\varepsilon_h$ from the quasidirect conduction band (CB) and valence band (VB) of Ge nanoclusters, respectively.

sidered to be trapped into the LCs upon excitation. Since they take part in FRET (schematically shown in Fig. 4) it is important to know the possible energy levels of $P1$ and $P2$. For quantitative analysis, we fit the PL quenching profiles by the modified Arrhenius equation,[29]

$$I = \frac{I_0}{\{1 + a_1 \exp(-\Delta\varepsilon_h/kT) + a_2 \exp[-(\Delta\varepsilon_h + \Delta\varepsilon_e)/kT]\}},$$

where $I_0 \propto G_c \tau_c / \Gamma$. Here, $\Delta\varepsilon_h$ and $\Delta\varepsilon_e$ represent the hole binding energy at a filled trap and the depth of the electron trap, while G_c, τ_c, and Γ denote the carrier generation rate, the carrier lifetime, and the total decay rate, respectively. The prefactors a_1 and a_2 can be expressed as $a_1 = \sigma_h/\Gamma_r$ and $a_2 = \sigma_e/\Gamma_r$, where σ_h and σ_e are the hole and electron capture rate constants, respectively, and Γ_r is the recombination rate. The fitted curves are superimposed on the experimental data (Fig. 4). Using the fitting procedure for S_{Ge}, the $\Delta\varepsilon_e$ and $\Delta\varepsilon_h$ are derived to be ~99 and ~19 meV for $P1$, while the respective values for $P2$ are found to be ~39 and ~9 meV. On the other hand for $S_{\mathrm{Ge+Er}}$, $\Delta\varepsilon_e$ and $\Delta\varepsilon_h$ are calculated to be ~43 and ~4 meV for $P1$ where they are ~61 and ~5 meV for $P2$, respectively. The systematic decrease in $\Delta\varepsilon_h$ and $\Delta\varepsilon_e$ values by introducing Er in S_{Ge} can be associated with the slightly different environment near the cluster/SiO_2 interface due to Er doping.

In summary, we present the PL behavior of the Er:Ge-NCs:SiO_2, exhibiting the 1.53 μm Er PL at RT in the presence of excess Ge. The PL intensity was found to increase as a function of Er concentration. With decreasing measurement temperature the 1.53 μm Er PL disappears and is replaced with the defect-related PL, which consists of two bands $P1$ and $P2$ within 1525 and 1440 nm. In addition, their intensity increases when the measuring temperature decreases from 150 to 15 K. Detailed spectral analyses suggest that the bands $P1$ and $P2$ are associated with luminescence centers near the Ge cluster/SiO_2 interface where the radiative recombination in these centers competes with the thermal redistribution of the localized excitons. Using time-resolved PL dynamics, this study further elucidates the temperature-dependent phonon-assisted Förster-type energy-transfer process from the luminescence centers to the Er^{3+} ions in Er:Ge-NCs:SiO_2 above 150 K. In our opinion, the present study provides a useful benchmark for future theoretical and experimental improvement of this photonic system.

The authors thank the Rossendorf Implantation Group for ion implantation and H. Felsmann, C. Neisser, and G. Schnabel for their careful semiconductor preparation work. This work was financially supported by the Alexander von Humboldt Foundation.

*Corresponding author. a.kanjilal@fzd.de

[1] O. Savchyn *et al.*, Phys. Rev. B **77**, 205438 (2008).
[2] B. Garrido *et al.*, Phys. Rev. B **76**, 245308 (2007).
[3] I. Izeddin *et al.*, Phys. Rev. Lett. **97**, 207401 (2006); D. Timmerman *et al.*, Nat. Photonics **2**, 105 (2008).
[4] C. L. Heng *et al.*, Appl. Phys. Lett. **85**, 4475 (2004).
[5] K. Das *et al.*, Nanotechnology **18**, 095704 (2007).
[6] A. Kanjilal *et al.*, J. Appl. Phys. **104**, 103522 (2008); D. Kuritsyn *et al.*, Appl. Phys. Lett. **83**, 4160 (2003).
[7] M. Ardyanian *et al.*, J. Appl. Phys. **102**, 106103 (2007).
[8] P. G. Kik *et al.*, Appl. Phys. Lett. **76**, 2325 (2000).
[9] J. F. Ziegler and J. P. Biersack, SRIM-2006.02, http://www.srim.org
[10] A. Janotta *et al.*, Phys. Rev. B **68**, 165207 (2003).
[11] A. Kanjilal *et al.*, Phys. Rev. B **79**, 161302(R) (2009).
[12] Y. M. Niquet *et al.*, Appl. Phys. Lett. **77**, 1182 (2000).
[13] T. Takagahara and K. Takeda, Phys. Rev. B **46**, 15578 (1992); C. Bulutay, *ibid.* **76**, 205321 (2007); G. Nesher *et al.*, *ibid.* **71**, 035344 (2005).
[14] S. Takeoka *et al.*, Phys. Rev. B **58**, 7921 (1998).
[15] G. H. Dieke, *Spectra and Energy Levels of Rare Earth Ions in Crystals* (Interscience Publishers, New York, 1968), Chap. 13.
[16] H. Z. Song and X. M. Bao, Phys. Rev. B **55**, 6988 (1997); K. Kajihara *et al.*, Appl. Phys. Lett. **79**, 1757 (2001).
[17] A. Kanjilal *et al.*, J. Appl. Phys. **106**, 026104 (2009).
[18] A. P. Li *et al.*, Phys. Rev. B **69**, 245310 (2004).
[19] V. A. Belyakov *et al.*, Adv. Opt. Technol. **2008**, 279502 (2008).
[20] M. Fujii *et al.*, Phys. Rev. B **72**, 165321 (2005).
[21] T. Förster, Naturwiss. **33**, 166 (1946); Ann. Phys. (N.Y.) **2**, 55 (1948).
[22] G. Allan and C. Delerue, Phys. Rev. B **75**, 195311 (2007).
[23] M. Fujii *et al.*, J. Appl. Phys. **95**, 272 (2004); K. Imakita *et al.*, Phys. Rev. B **71**, 193301 (2005).
[24] T. Miyakawa and D. L. Dexter, Phys. Rev. B **1**, 2961 (1970).
[25] V. Kveder and M. Kittler, Mater. Sci. Forum **590**, 29 (2008).
[26] J. I. Pankove, *Optical Processes in Semiconductors* (Prentice-Hall, Englewood, NJ, 1971), p. 25; Y. P. Varshni, Physica (Amsterdam) **34**, 149 (1967); S. Fukatsu *et al.*, Appl. Phys. Lett. **68**, 1889 (1996).
[27] A. Kanjilal *et al.*, Appl. Phys. Lett. **94**, 051903 (2009).
[28] A. Kanjilal *et al.*, J. Appl. Phys. **106**, 063112 (2009); L. Rebohle *et al.*, Appl. Phys. B: Lasers Opt. **71**, 131 (2000).
[29] P. G. Kik *et al.*, Appl. Phys. Lett. **70**, 1721 (1997).